

# A SIMPLE PARAMETERISATION FOR FLUX FOOTPRINT PREDICTIONS

N. KLJUN\*

*Institute for Atmospheric and Climate Science ETH, Zurich, Switzerland*

P. CALANCA

*Swiss Federal Research Station for Agroecology and Agriculture, Zurich, Switzerland*

M. W. ROTACH\*\*

*Institute for Atmospheric and Climate Science ETH, Zurich, Switzerland*

H. P. SCHMID

*Department of Geography, Indiana University, Bloomington, U.S.A.*

(Received in final form 19 November 2003)

**Abstract.** Flux footprint functions estimate the location and relative importance of passive scalar sources influencing flux measurements at a given receptor height. These footprint estimates strongly vary in size, depending on receptor height, atmospheric stability, and surface roughness. Reliable footprint calculations from, e.g., Lagrangian stochastic models or large-eddy simulations are computationally expensive and cannot readily be computed for long-term observational programs. To facilitate more accessible footprint estimates, a scaling procedure is introduced for flux footprint functions over a range of stratifications from convective to stable, and receptor heights ranging from near the surface to the middle of the boundary layer. It is shown that, when applying this scaling procedure, footprint estimates collapse to an ensemble of similar curves. A simple parameterisation for the scaled footprint estimates is presented. This parameterisation accounts for the influence of the roughness length on the footprint and allows for a quick but precise algebraic footprint estimation.

**Keywords:** Boundary-layer scaling, Boundary-layer stability, Fetch, Flux footprint, Lagrangian stochastic particle dispersion model, Parameterisation.

## 1. Introduction

The surface area of influence for surface-atmosphere exchange is of special interest for the design of observation programs and for the interpretation of trace gas flux measurements. The area containing the effective surface sources and sinks contributing to a given measurement point can be estimated and weighted by so-called footprint models. The footprint function estimates the probability of a passive scalar emitted at such a source location to contribute to the turbulent flux at the receptor position. In recent years, a variety of footprint models have been presented, using analytical, stochastic, or numerical approaches in Eulerian or Lagrangian

\* E-mail: nkljun@ethz.ch

\*\* Present affiliation: Swiss Federal Office of Meteorology and Climatology, MeteoSwiss, Zurich, Switzerland.



frameworks. A detailed review of these different footprint approaches and their applications can be found in Schmid (2002).

Long-term and short-term observations are regularly exposed to different atmospheric conditions and therefore involve an enormous number of footprint calculations. Footprint models based on Lagrangian and large-eddy simulation (LES) are often highly CPU-intensive and therefore usually not suited to this type of application. Analytical models, on the other hand, are simple to compute but often invalid for many of the observed conditions. Existing footprint modelling studies offer the potential for simple parameterisations as, for example, proposed by Horst and Weil (1992, 1994), Weil and Horst (1992), Schmid (1994) or Hsieh et al. (2000). The primary drawback of these parameterisations is their limitation to a particular turbulence scaling domain (often Monin–Obukhov similarity and surface-layer scaling), or to a limited range of stratifications. Conversely, measurement programs of even just a few days are regularly exposed to conditions spanning several turbulence scaling domains.

In the present study, a scaling procedure is suggested for the crosswind-integrated flux footprint based on a few basic variables easily derived from common turbulence measurements (Section 2). This scaling approach is applied to flux footprint estimates obtained from a thoroughly tested Lagrangian footprint model (Kljun et al., 2002). It is shown that scaled footprint estimates for a wide range of stabilities and receptor heights within or above the surface layer collapse to a set of self-similar curves depending only on the roughness length (Section 3). A simple parameterisation of the ensemble of scaled footprint estimates is proposed in Section 4, accounting for the dependence of the footprint on the roughness length. Some applications of the scaling procedure and its parameterisation are presented in Section 5.

## 2. Scaling Parameters

In a physical sense, the near limit of the flux footprint is given by the requirement that emitted trace gas particles have enough time to attain the receptor height,  $z_m$ , and contribute to the flux before being advected downstream. Particles arriving at the receptor from sources beyond the far limit have lost any correlation with the source and thus do not contribute to the net flux (i.e., their vertical velocity distribution has a zero mean (Wilson and Swatters, 1991). Keeping these limits of the footprint in mind, its extent consequently is highly dependent on the receptor height (Weil and Horst, 1992; Schmid, 1994), but also on the turbulence in which the scalar is dispersed. Thus, the footprint size and shape depends on the ratio of advection to (thermal and mechanical) turbulent transport, which varies with the stability regime and surface properties. Ideally, a scaling procedure should consider variables that describe these factors explicitly, but can, at the same time, easily be determined from measurements.

For the crosswind-integrated footprint function,  $\overline{f^y}$ , the relevant length scales are the alongwind distance from the receptor,  $x$ , the receptor height,  $z_m$ , and the planetary boundary-layer (PBL) height,  $h$ , which represents the largest eddy scale responsible for the flux. The dependence of the footprint on the stability regime is more complex, as there is a wide variety of variables that could be chosen as key variables. Near the ground, turbulence is generated by wind shear. For the advection and diffusion of particles in this region, the surface friction velocity,  $u_*$ , is the key scaling velocity. Buoyant processes throughout the PBL can be described by the standard deviation of vertical velocity fluctuations,  $\sigma_w$ . This scale is important for characterising the vertical dispersion strength and hence the size of the footprint. Here,  $\sigma_w$  is preferable over the Deardorff velocity scale,  $w_*$ , as the latter is not defined for the stable boundary layer.

Based on these considerations,  $\overline{f^y}$  can be regarded as a yet unspecified function of  $x$ ,  $z_m$ ,  $h$ ,  $u_*$ , and  $\sigma_w$ . According to the Buckingham  $\Pi$  Theorem (Stull, 1988), four dimensionless combinations ( $\Pi$  groups) can be found to, in the most general case, reformulate the above function as  $\Pi_1 = f(\Pi_2, \Pi_3, \Pi_4)$ . A possible set of initial  $\Pi$  groups is

$$\Pi_1 = z_m \overline{f^y}, \quad (1)$$

$$\Pi_2 = x/z_m, \quad (2)$$

$$\Pi_3 = h/z_m, \quad (3)$$

$$\Pi_4 = \sigma_w/u_*. \quad (4)$$

$\Pi_3$  exhibits a strong variation if  $h$  is small, i.e., in stable conditions, or if  $z_m$  is very large.  $\Pi_4$ , on the other hand, is one possibility of taking the ratio of thermally and mechanically induced turbulent transport into account (see also Miyake (1965)).  $\Pi_4$  varies with height for strongly convective conditions, but is nearly invariant in neutral or stable stratification.

Based on experimental results, the vertical variation of turbulent fluxes due to a horizontally homogeneous surface source of infinite extent can be described as a function of the height,  $z$ . This linear function holds maximum values at the surface and decreases towards the top of the PBL, where (neglecting entrainment) the fluxes are assumed to vanish (Stull, 1988). Assuming that the same holds true for the flux footprint, it is thus preferable to modify  $\Pi_3$  to form  $\Pi'_3 = h/(h - z_m)$ .

The aim of this scaling exercise is clearly to express a non-dimensional form of the crosswind-integrated footprint function,  $F_*$ , as a function of a non-dimensional alongwind distance,  $X_*$ , in a form  $\Pi_1 = f(\Pi_2, \Pi_3, \Pi_4)$ . Here, it is postulated that  $X_*$  and  $F_*$  can be formed as linear combinations of the above  $\Pi$  groups,  $X_* = \Pi_4^{\alpha_1} \Pi_2$  and  $F_* = \Pi_4^{\alpha_2} \Pi'_3 \Pi_1$ . Explicitly,

$$X_* = \left( \frac{\sigma_w}{u_*} \right)^{\alpha_1} \frac{x}{z_m}, \quad (5)$$

$$F_* = \left( \frac{\sigma_w}{u_*} \right)^{\alpha_2} \left( 1 - \frac{z_m}{h} \right)^{-1} z_m \overline{f^y}, \quad (6)$$

where  $\alpha_1$  and  $\alpha_2$  are introduced as free parameters. It will be shown below (Subsection 3.2) that data from footprint simulations for varying stability conditions and receptor heights attest to the usefulness of Equations (5) and (6) and that a simple power-law dependence captures the essential variations of the footprints on  $\Pi_4$ . Within the surface layer, the present scaling is consistent with the one proposed by Horst and Weil (1992) (cf. Appendix A.1).

$X_*$  and  $F_*$  retain a dependence on the surface roughness length,  $z_0$  (Subsection 3.3). The roughness length can be seen as representing the strength of the surface as a momentum sink and shear generated turbulence. However, to avoid an overabundance of length scales in the present scaling scheme, the roughness length is excluded from the set of fundamental scaling quantities and its influence is addressed in the parameterisation of the scaled footprint estimates (Section 4).

### 3. Scaled Footprint Representation

Ideally, the present scaling procedure should be tested against observations. However, the availability of applicable experimental datasets is very limited so far. Thus, Equations (5) and (6) were investigated on the basis of footprint simulations.

#### 3.1. MODEL STRATEGY

Footprint estimates were derived using the three-dimensional Lagrangian stochastic footprint model LPDM-B of Kljun et al. (2002). This model satisfies the well-mixed condition continuously for convective to stable stratifications and for measurement heights (receptors) within or above the surface layer. Its dispersion module is based on the three-dimensional Lagrangian stochastic particle dispersion model developed by Rotach et al. (1996) and de Haan and Rotach (1998) and has been shown to successfully reproduce results of LES, water-tank and field data across a wide range of atmospheric stratification (Rotach et al., 1996; Rotach, 2001b). For a description of LPDM-B, see Kljun et al. (2002a).

Using LPDM-B, a first set of twenty-eight simulations was carried out for scenarios representing a broad range of stability conditions from strongly stable to strongly convective and receptor heights from close to the ground to far into the boundary layer (Table I). For this first set, the roughness length was set to a value corresponding to short grass. In a second step, another forty-eight simulations were carried out in order to analyse the influence of the surface roughness. Here, the roughness length was set to values representing farmland and forest canopies. For all simulations, the values of  $\sigma_w(z_m)$  were derived from the model inputs given in Table I according to the LPDM-B formulations. The receptor position was set to  $(0, 0, z_m)$ .

TABLE I

Velocity scales, Obukhov length, and PBL height describing the stability regimes of the selected scenarios.

Scenario	$u_*$ [ $\text{m s}^{-1}$ ]	$w_*$ [ $\text{m s}^{-1}$ ]	$L$ [m]	$h$ [m]
1 Strongly convective	0.2	2.0	-5	2000
2 Forced convective	0.2	1.0	-30	1500
3 Slightly convective	0.3	0.5	-650	1200
4 Neutral	0.5	0.0	$\infty$	1000
5 Slightly stable	0.4	-	1000	800
6 Stable	0.3	-	130	250
7 Strongly stable	0.3	-	84	200

Receptor heights at  $z_m/h = [0.005, 0.075, 0.25, 0.50]$

Roughness length  $z_0 = [0.01, 0.1, 0.3, 1.0]$  m

### 3.2. SCALED FOOTPRINTS FOR A GIVEN SURFACE ROUGHNESS

The crosswind-integrated flux footprints for a roughness length of  $z_0 = 0.01$  m (other values for the roughness length will be discussed below) are displayed in Figure 1. These plots clearly demonstrate the impact of receptor height and stability on the footprint size. The along-wind distance between receptor and peak location varies by four orders of magnitude, the footprint values by three. Note that in Figure 1, the peak values of the footprint for the stable cases are larger and the peak location closer to the receptor than for the convective cases. This is due to the fact that the footprint estimates are grouped according to the dimensionless height  $z_m/h$ . In the present scenarios, a change in stability also affected the height of the boundary layer. Thus, a particular dimensionless height,  $z_m/h$ , corresponded to a much smaller effective receptor height,  $z_m$ , in stable conditions than in the convective boundary-layer scenarios (Table I).

Using the simulations of LPDM-B, a linear relation among the  $\Pi$  groups was found when setting  $\alpha_1 = -\alpha_2 = 0.8$  (see Figure 2 for selected points of the simulations, namely the footprint peak location,  $x_{\max}$ , and the peak value,  $\overline{f^y}_{\max}$ ). In Figure 3, the footprint predictions of LPDM-B from Figure 1 are replotted in terms of  $X_*$  and  $F_*$ . In this representation, the scaled footprint estimates within the same roughness regime are closely clustered and collapse to an ensemble of similar curves. The peak location and the extent of the scaled footprint agree to a very high degree throughout all the simulations. These results suggest that the formulation of a single empirical  $F_*(X_*)$ -curve is justified. If the scaled footprint estimates are depicted for each stability regime separately, their coincidence is better for convective cases than for neutral or stable cases (not shown). This points

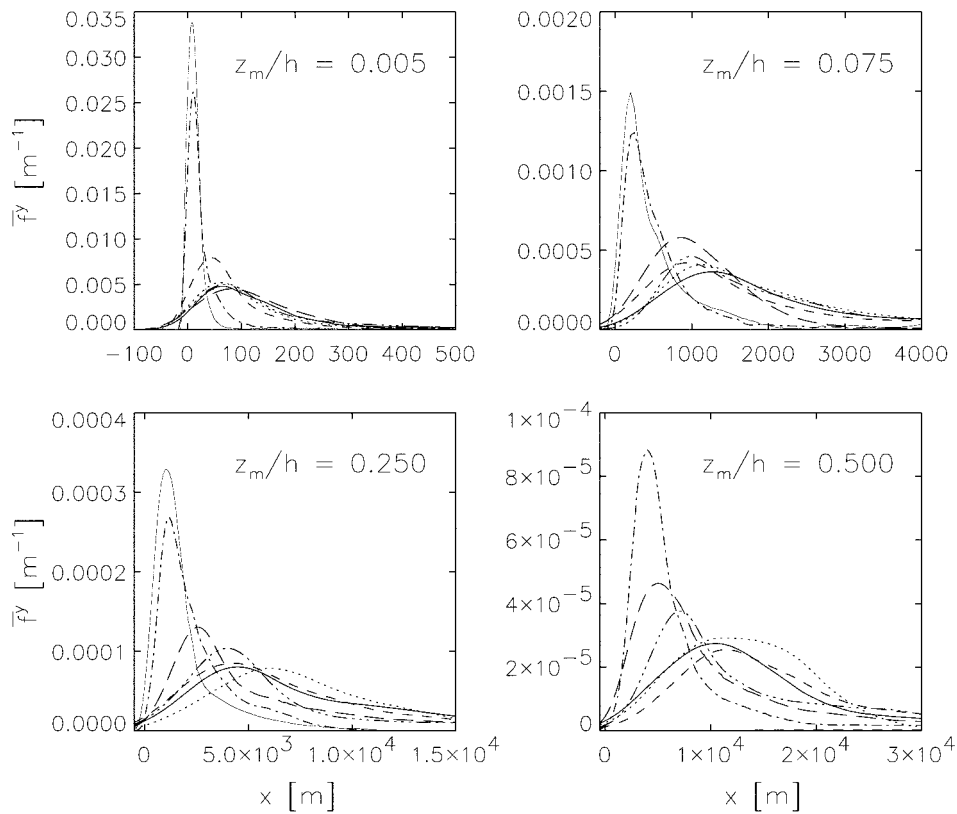


Figure 1. Crosswind-integrated flux footprint predictions in seven different stability regimes (see Table I) for four different receptor heights (as denoted in each panel) and a roughness length of  $z_0 = 0.01$  m. Stability conditions: strongly convective (---), forced convective (-·-·-), slightly convective (—), neutral (···), slightly stable (- - -), stable (-·-), and strongly stable (—, thin line). Note the varying ranges on both axes from panel to panel.

to a possible refinement of the scaling procedure in neutral and stable boundary layers when shear-generated turbulence is more important.

In practice, the present scaling procedure can be readily applied to describe changes in the footprint due to variations in stability, once a footprint for a given site (i.e., roughness length and measurement height) and one particular stability has been obtained by a suitable model. Thus, as a first result, this study provides an easy tool to estimate footprint variations for long-term observation programs at a given site, without the need to re-compute the footprint for every observation period.

### 3.3. INFLUENCE OF THE ROUGHNESS LENGTH ON SCALED FOOTPRINTS

The influence of the surface roughness on the footprint estimates and their scaled representation was examined by means of footprint predictions of LPDM-B for

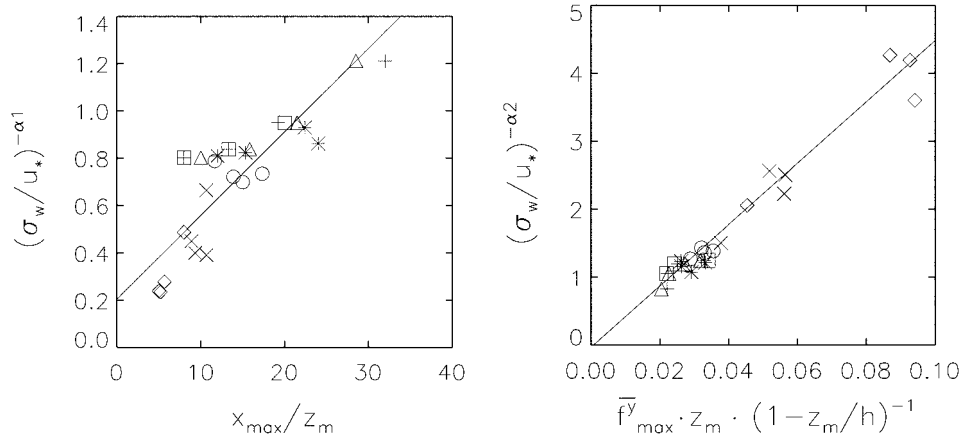


Figure 2. Relation between specific  $\Pi$  groups. Data as given by the scenarios of Table I.  $x_{\max}$  denotes the peak location and  $\bar{f}_{\max}^y$  the peak value of the footprint estimates. Stability conditions: strongly convective ( $\diamond$ ), forced convective ( $\times$ ), slightly convective ( $\circ$ ), neutral ( $*$ ), slightly stable ( $\Delta$ ), stable ( $+$ ), and strongly stable ( $\square$ ), roughness length  $z_0 = 0.01$  m. The solid lines denote the linear fit obtained after setting  $\alpha_1 = -\alpha_2 = 0.8$ .

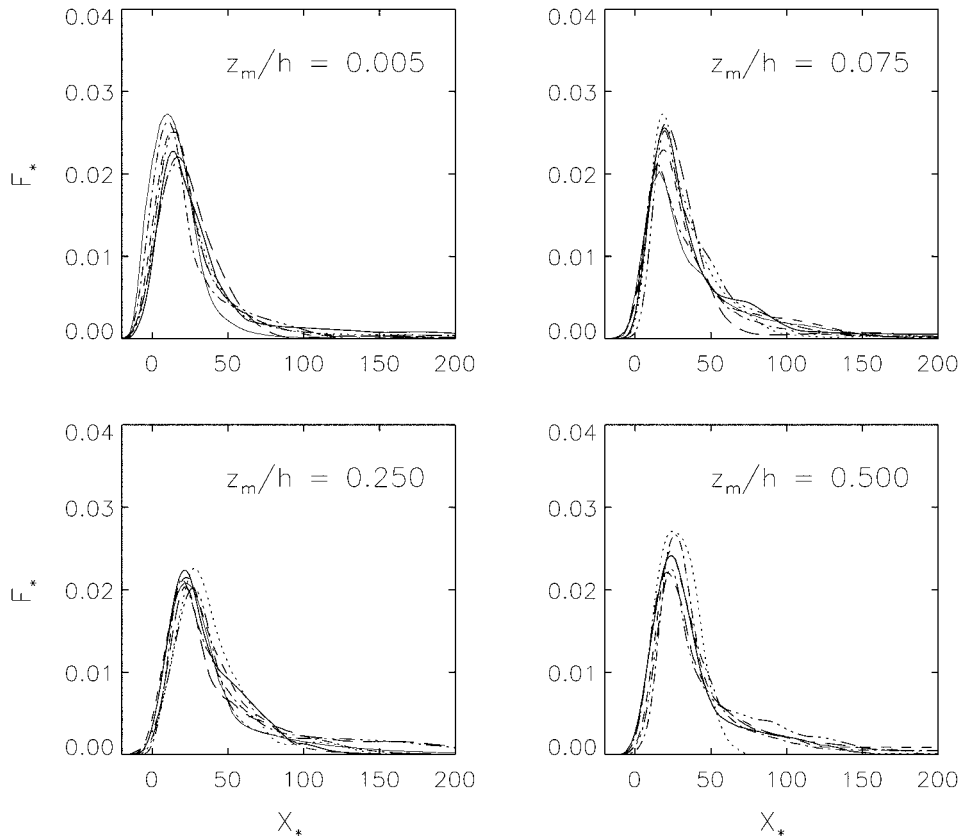


Figure 3. Same as Figure 1, but for scaled crosswind-integrated flux footprints.

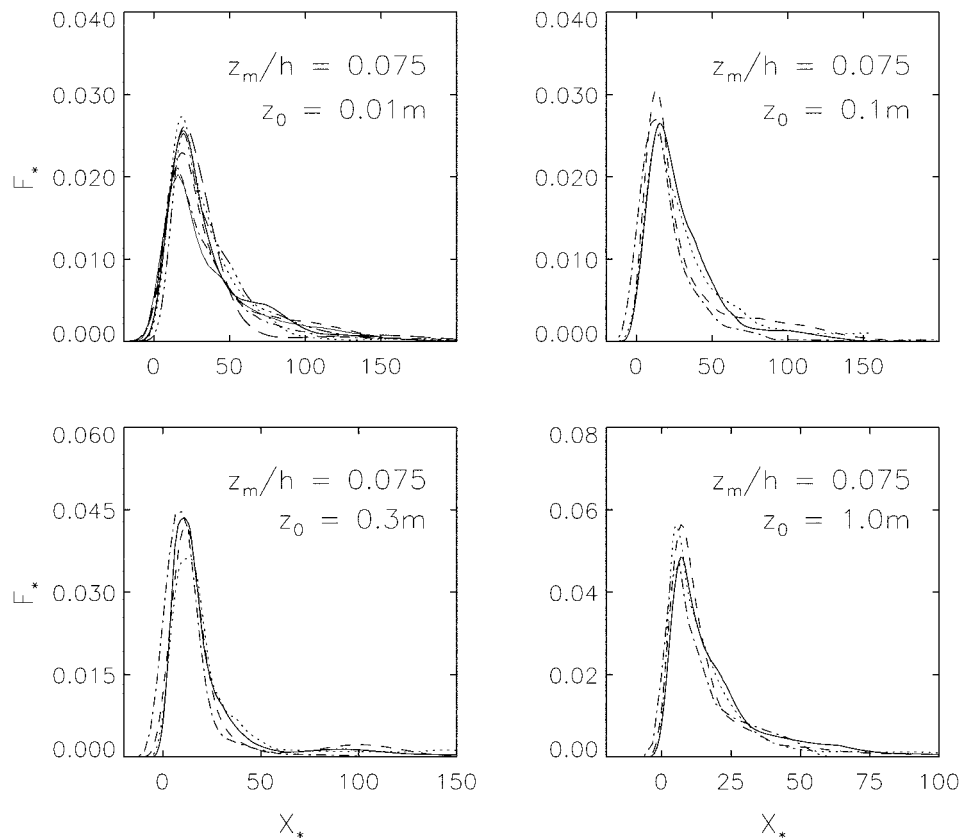


Figure 4. Scaled crosswind-integrated flux footprints for a receptor height of  $z_m/h = 0.075$  and a roughness length as indicated in each panel. Stability conditions: strongly convective (—), forced convective (— · ·), slightly convective (—), neutral (· · ·), slightly stable (- - -), stable (- ·), and strongly stable (—, thin line). Note the different ranges on both axes.

roughness length values of  $z_0 = [0.01, 0.1, 0.3, 1.0]$  m. For high values of  $z_0$ , the depth of the roughness sublayer is no longer negligible. Similar to most footprint models, roughness sublayer turbulence is not implemented in LPDM-B, and thus, receptor heights within the latter were not considered in this study. The depth of the roughness sublayer,  $z_*$ , was estimated as  $z_* = 2h_r$  to  $5h_r \approx 16z_0$  to  $39z_0$ ,  $h_r$  being the mean height of the roughness elements (Raupach et al., 1991). As suggested by Rotach (2001a), Raupach's higher limit of  $z_*$  was selected for  $z_0 = 0.01$  m, while for all other values of the roughness length,  $z_*$  was set to Raupach's lower limit.

Again, the free parameters  $\alpha_1$  and  $\alpha_2$  were determined using the respective simulations of LPDM-B. It was found that the free parameters do not depend on the roughness length. As shown in Figure 4, similarity of the scaled footprints is preserved for each value of the roughness length. With increasing  $z_0$ , the dis-

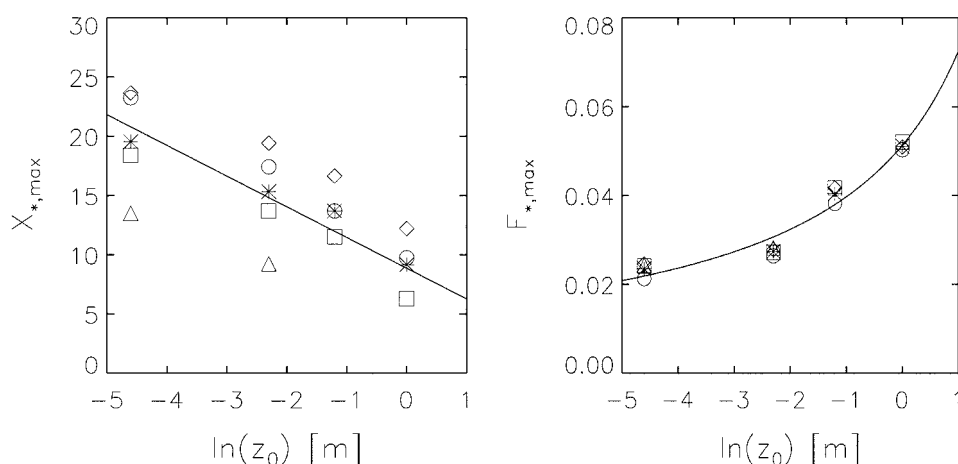


Figure 5. Dependence of the peak location,  $X_{*,max}$ , and peak value,  $F_{*,max}$ , of the scaled footprint estimates on the roughness length,  $z_0$ . These footprint estimates range from strongly convective to strongly stable (Table I) with receptor heights of  $z_m/h = [0.005 (\Delta), 0.075 (\square), 0.25 (\circ), 0.50 (\diamond)]$  and an average of all receptor heights ( $*$ ). Solid lines represent a fit according to Equations (11) and (12) (see Section 4).

tance between the receptor and the peak location of the scaled footprint estimates,  $X_{*,max}$ , decreases, while the peak value,  $F_{*,max}$ , increases and the shape of the curve narrows (Figure 5). The variability of the size of scaled footprint estimates with roughness length is due to the enhanced mechanical turbulence over rougher surfaces. Thus, Figures 3, 4, and 5 reveal that the similarity analysis does not lead to a truly universal function  $F_*(X_*)$ . However, in order to consider only measurable variables in the scaling procedure, the dependence of the scaled footprint on the roughness length was not included in Equations (5) and (6) but was implemented in the parameterisation (Section 4).

### 3.4. FURTHER TESTS AND RESTRICTIONS

The success of the scaling procedure presented in the previous sections raises the question whether the quality of the results could be due to the specific setup of LPDM-B. Therefore, as a further test, the scaling procedure was also applied to footprint estimates of the analytical footprint model of Kormann and Meixner (2001). This model is similar to those of Horst and Weil (1992, 1994) or Schmid (1994) in that it is based on the diffusion model of Van Ulden (1978). See Kljun et al. (2003) for a direct comparison of its predictions with LPDM-B's results. To ensure the applicability of the analytical model, the test was restricted to scenarios of moderate stratification within the surface layer (scenarios 3 to 5 of Table I for receptor heights at  $z_m/h = [0.005, 0.075]$  and a roughness length of  $z_0 = 0.01$  m). When applying the scaling procedure, the scaled footprint estimates from the analytical model also collapsed into a group of similar curves (not shown).

In order to assess the limits of the dimensionless footprint approach, further simulations with LPDM-B were carried out. The simulations were designed to cover extreme conditions: the receptor height was set between 0.5 and 1250 m, the boundary-layer height was varied between 100 and 2,500 m, and the boundary-layer stability conditions were defined according to  $-13,000 < z_m/L < 2.4$ . Values for  $u_*$  were set in the range of 0.05 and 0.5  $\text{m s}^{-1}$ , whereas  $\sigma_w$  was chosen to range between 0.23 and 1.23  $\text{m s}^{-1}$ . It was found that in conditions of extremely strong convection ( $z_m/L < -200$  and  $u_* < 0.2 \text{ m s}^{-1}$ ), the similarity of the resulting scaled footprint estimates for different receptor heights was preserved, but the scaled footprint estimates were shifted further downwind of the receptor location than the ensemble footprint curve for more moderate conditions. Thus, even though the scaling procedure did not explicitly fail for such extremely convective conditions, the size and location of the scaled footprint did not agree with those obtained for  $u_* > 0.2 \text{ m s}^{-1}$ . In stable conditions, the scaling procedure was found to hold when stability was limited to  $z_m/L \leq 1$ . According to the LPDM-B simulations, the overall conditions for the validity of the scaling procedure (within the atmospheric boundary layer and dynamically homogeneous terrain) can be formulated as  $-200 \leq z_m/L \leq 1$ ,  $u_* \geq 0.2 \text{ m s}^{-1}$ ,  $z_m > 1 \text{ m}$ .

At this point it has to be re-emphasised that the scaling procedure and its validity range were not derived from real-world observations but from a model. Even though LPDM-B is highly suited for footprint calculations, it is still an abstraction of processes in the real atmosphere. In addition, it is possible that conditions outside the above limits are encountered. For such cases, it would be essential to run specific simulations using a full footprint model.

#### 4. Parameterisation

As a next step, a functional relation between  $F_*$  and  $X_*$  was sought. The following equation successfully describes the ensemble of scaled footprint estimates within one roughness regime

$$\hat{F}_* = a \left( \frac{\hat{X}_* + d}{c} \right)^b \exp \left\{ b \left( 1 - \frac{\hat{X}_* + d}{c} \right) \right\}. \quad (7)$$

Equation (7) is formally similar to the analytical footprint equation proposed by Kormann and Meixner (2001). Here,  $a$ ,  $b$ ,  $c$ , and  $d$  are fitting parameters, and  $\hat{F}_*(\hat{X}_*)$  is the parameterisation of  $F_*(X_*)$  with the property that

$$\hat{X}_{*,\max} = c - d, \quad (8)$$

$$\hat{F}_{*,\max} = a, \quad (9)$$

TABLE II

Optimal values for the parameters of Equation (7) based on a fit to the scaled footprint estimates depicted in Figures 3 and 4. The parameters for  $z_0 = [0.1, 0.3, 1.0]$  m are based on a reduced set of model runs (e.g., receptor heights within the roughness sublayer were omitted).

$z_m/h$	$z_0 = 0.01$ m				$z_0 = 0.1$ m			
	$a$	$b$	$c$	$d$	$a$	$b$	$c$	$d$
0.005	0.024	3.84	31	18	0.028	2.47	22	12
0.075	0.024	4.11	33	15	0.027	2.87	24	10
0.250	0.021	3.61	35	12	0.026	3.40	27	10
0.500	0.025	4.23	33	9	0.028	5.06	32	12
all $z_m$ 's	0.024	4.21	34	15	0.027	3.56	27	12
$z_m/h$	$z_0 = 0.3$ m				$z_0 = 1.0$ m			
	$a$	$b$	$c$	$d$	$a$	$b$	$c$	$d$
0.075	0.042	4.06	19	7	0.052	2.40	11	5
0.250	0.038	4.24	21	7	0.050	3.19	14	4
0.500	0.042	6.02	23	6	0.051	3.93	15	3
all $z_m$ 's	0.040	5.08	22	8	0.051	3.35	14	5

where,  $\hat{X}_{*,\max}$  denotes the peak location and  $\hat{F}_{*,\max}$  the peak value of the parameterisation. The application of Equation (7) is restricted to  $\hat{X}_* > -d$ . Thus, unlike the scaled footprint itself, the parameterised footprint does not extend to  $-\infty$ . Equation (7) must also satisfy the integral condition, which reads (see e.g., Schmid, 1994)

$$\int_{-d}^{\infty} \hat{F}_* d\hat{X}_* = ac \exp(b)b^{-b}\Gamma(b) = 1, \tag{10}$$

where  $\Gamma$  is the gamma function (see Appendix A.2 for a derivation of the integral function). The parameters  $a$ ,  $b$ ,  $c$ , and  $d$  can be found from fitting Equations (7) to (10) to the scaled footprint ensemble (stepwise regression). Table II summarises the values of  $a$ ,  $b$ ,  $c$ , and  $d$  for the footprints of LPDM-B in the scenarios of Table I. The parameterisations based on  $a$ ,  $b$ ,  $c$ , and  $d$  as in Table II for all receptor heights and roughness lengths are shown in Figure 6.

The quality of the parameterisation was estimated by determining correlation (CORR), fractional bias (FB), and normalised mean square error (NMSE) following Hanna et al. (1993). For the peak location, NMSE and FB were of the order of 0.05 and CORR between 0.93 and 0.99. For the whole footprint curve, NMSE was of the order of 0.35, FB around 0.00, and CORR between 0.92 and 0.96. For a

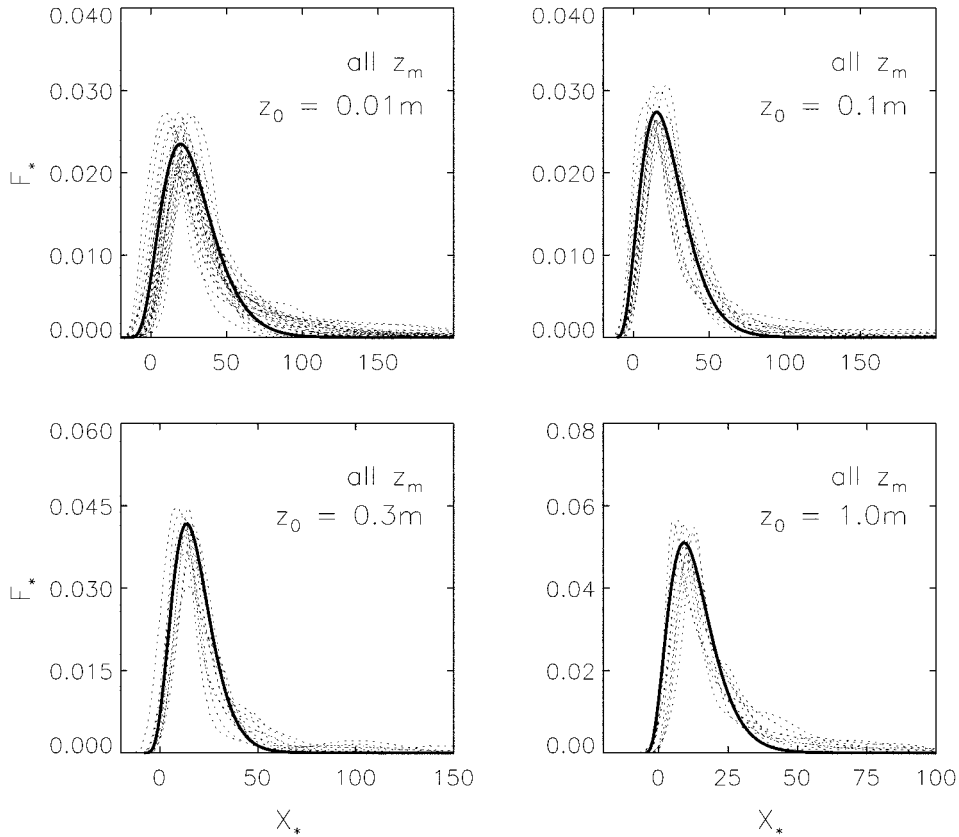


Figure 6. Parameterisation of the ensemble of scaled flux footprints (Equation (7), solid line). The dashed lines indicate the scaled footprint estimates (LPDM-B simulations). These footprint estimates range from strongly convective to strongly stable (Table I) with receptor heights of  $z_m/h = [0.005, 0.075, 0.25, 0.50]$ . Roughness length as indicated in each panel.

simple, easy-to-apply footprint parameterisation rather than a highly sophisticated prediction, the parameterisation based on the fit over all receptor heights (Table II) serves its purpose well. For a more specific prediction, the parameterisation can simply be fitted to selected scaled footprint estimates (i.e., taking into account the receptor height of a specific experimental site).

Table II also reveals the dependence of the fitting parameters,  $a$ ,  $b$ ,  $c$ ,  $d$ , on the roughness length and hence indicates again the dependence of  $F_*$  and  $X_*$ , or of  $\hat{F}_*$  and  $\hat{X}_*$ , on the latter. In Subsection 3.3 (Figure 5), it already has been shown that  $X_{*,\max}$  and  $F_{*,\max}$  are functions of  $\ln(z_0)$ . In analogy to the surface-layer model of Horst and Weil (1992), this dependence can be described as follows (see Appendix A.1 for a derivation)

$$\hat{X}_{*,\max} \approx A_X(B - \ln z_0), \quad (11)$$

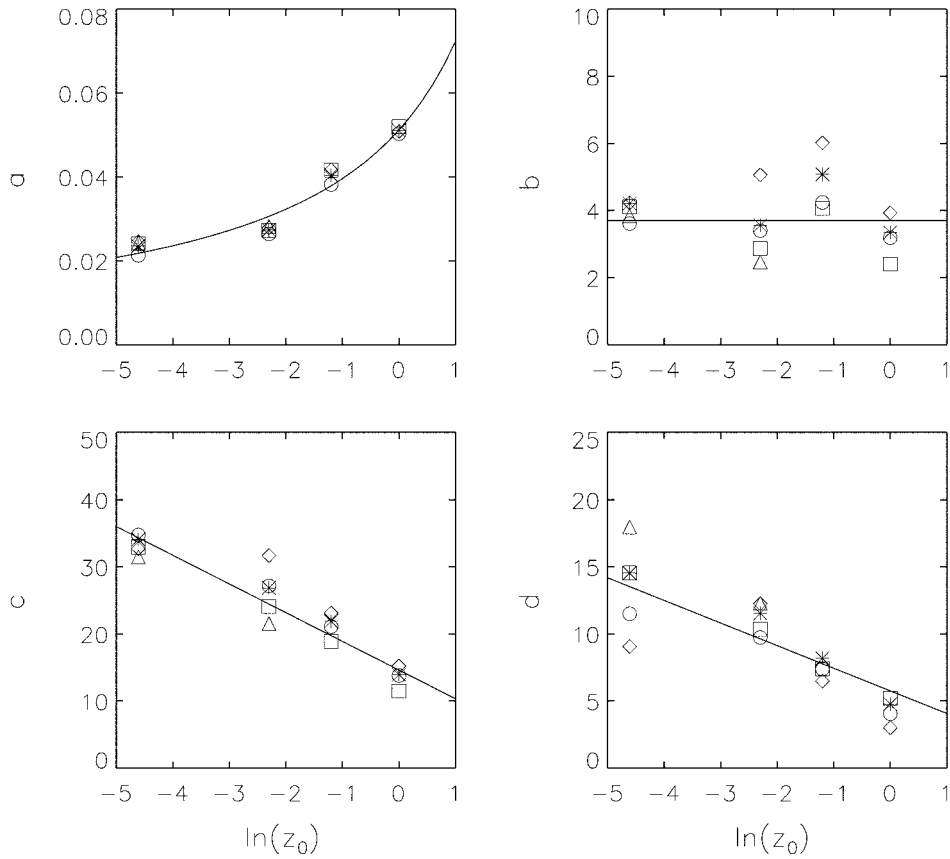


Figure 7. Dependence of the fitting parameters,  $a$ ,  $b$ ,  $c$ ,  $d$ , on the roughness length,  $z_0$ , for footprint estimates ranging from strongly convective to strongly stable (Table I) with receptor heights of  $z_m/h = [0.005 (\Delta), 0.075 (\square), 0.25 (o), 0.50 (\diamond)]$  and an average of all receptor heights ( $*$ ). Solid lines represent a fit according to Equations (13) to (16), respectively.

$$\hat{F}_{*,\max} \approx \frac{A_F}{(B - \ln z_0)}. \tag{12}$$

The parameters  $A_X$ ,  $B$ , and  $A_F$  are approximately constant. Applying Equations (8) to (10), the above equations can be extended to provide an interpolation framework for  $a$ ,  $c$ , and  $d$  for those values of the roughness length,  $z_0$ , not covered by the present scenarios

$$a \approx \frac{A_F}{(B - \ln z_0)}, \tag{13}$$

$$\exp(b)b^{-b}\Gamma(b) = \frac{1}{ac} \approx \frac{1}{A_F A_C} \approx \text{constant}, \tag{14}$$

$$c \approx A_C(B - \ln z_0), \tag{15}$$

$$d \approx A_D(B - \ln z_0), \quad (16)$$

where  $A_F$ ,  $B$ ,  $A_C$ , and  $A_D$  are constant parameters. Fitting the above equations to the optimal values of the footprint parameterisation of Table II yields  $A_X = 2.59 \pm 0.17$ ,  $B = 3.42 \pm 0.35$ ,  $A_F = 0.18 \pm 0.01$ ,  $A_C = 4.28 \pm 0.13$ ,  $A_D = 1.68 \pm 0.11$ , and  $b = 3.70 \pm 0.30$ , suggesting the latter to be approximately constant (Figure 7). If  $a$ ,  $b$ ,  $c$ , and  $d$  are computed from the above equations, the parameterisation (tested by means of CORR, FB, and NMSE with respect to the LPDM-B simulations) is almost of the same quality as the parameterisation determined by the parameter values of Table II. Using Equations (13) to (16), it is thus straightforward to derive a parameterised scaled footprint, which allows estimation of the ‘real-scale’ footprint for almost any roughness length and a broad range of stability conditions and receptor heights. However, it clearly has to be kept in mind that the parameters were not derived from real-world observations but from a model, a model that is highly suited for such calculations but of course still bears some idealisations.

Footprint estimates of the present parameterisation were compared with corresponding estimates of Hsieh et al. (2000), who also used results of a Lagrangian stochastic dispersion model to derive a footprint parameterisation. Their model differs from LPDM-B in that it is one-dimensional and based on Gaussian turbulence. Unlike in LPDM-B, the skewness of the vertical velocity, the covariance  $\overline{u'w'}$ , as well as the longitudinal turbulence, are not considered in their model. Hsieh et al. (2000) derived a scaling procedure for the streamwise extent of the footprint and, using their model results, obtained a parameterisation for footprint estimates. The derivation of their approach depends in several aspects, explicitly or implicitly, on surface-layer assumptions and on neutrality. When comparing footprint estimates derived from the two parameterisations, satisfactory agreement was found for near-neutral and near-surface conditions (not shown). For receptors higher than 20 m and conditions outside a moderate stability range (scenarios 1, 2, 6, 7, Table I), however, the peak location as estimated by the two approaches differed considerably (not shown). This discrepancy is attributed to the differences between the two models as outlined above and possibly the very limited range of modelled receptor heights (2–20 m) that Hsieh et al. (2000) used to derive their parameters. Since the parameters of the present parameterisation are based on model results computed from a footprint model, which is suited for a wide range of stability conditions and receptor heights, its results are likely more generally valid.

## 5. Applications

For the design of a field study and for the interpretation of trace gas flux measurements, the peak location and the longitudinal dimension of the footprint estimate (fetch) are of special interest. The present footprint parameterisation allows rapid

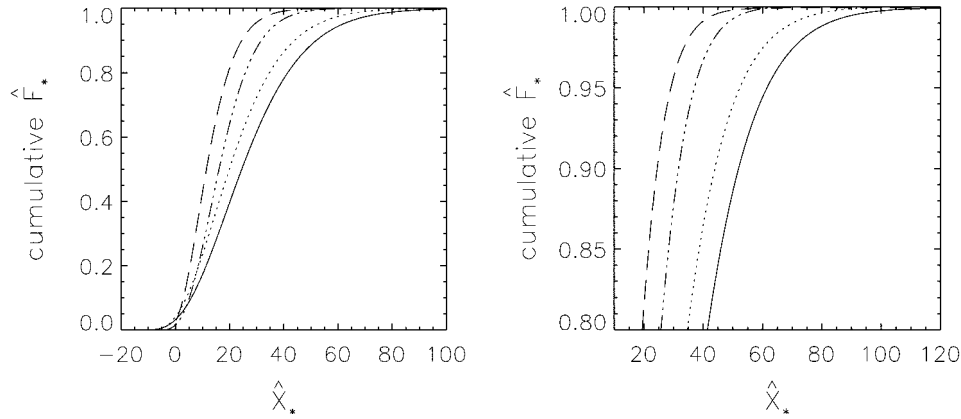


Figure 8. Cumulative form of the footprint parameterisation,  $\hat{F}_*$ , as a function of the distance from the receptor,  $\hat{X}_*$ . Displayed are the parameterisations for the present scenarios (Table I) including all receptor heights and a roughness length of  $z_0 = [0.01$  (—),  $0.1$  (···),  $0.3$  (- · - ·),  $1.0$  (- -)] m. The right-hand panel is zoomed into the upper part of the left-hand panel.

assessment of these footprint characteristics with the advantage of being valid also outside the surface layer.

Given the peak location of the scaled footprint estimate or of the present footprint parameterisation (Equation (8) and Table II or Equation (11)), the peak location of the footprint in a dimensional framework,  $x_{\max}$ , can be found from Equation (5) as

$$x_{\max} = X_{*,\max} z_m \left( \frac{\sigma_w}{u_*} \right)^{-\alpha_1} . \tag{17}$$

Next, Equation (7) can be integrated to derive a cumulative form of the footprint parameterisation (see Appendix A.2). Such cumulative footprints are depicted in Figure 8 for different values of the roughness length. The footprint estimate cumulated to a selected threshold reflects the percentage,  $R$ , of the scaled footprint included within a certain scaled distance,  $\hat{X}_{*,R}$ , from the receptor. This distance can be derived by means of partial integration of Equation (7) (see Appendix A.2) or directly from Figure 8. As can be seen from Figure 6, the parameterisation for large values of  $X_*$  (ratio of cumulative footprint  $R > 95\%$ ) does not represent the scaled footprint ensembles as well as for smaller values. It is therefore not recommended to compute  $\hat{X}_{*,R}$  for values of  $R$  larger than 95%. Finally, applying Equation (5) to the scaled distance,  $\hat{X}_{*,R}$ , yields the longitudinal dimension of the footprint,  $x_R$ , in the original non-scaled frame

$$x_R \approx \hat{X}_{*,R} z_m \left( \frac{\sigma_w}{u_*} \right)^{-\alpha_1} . \tag{18}$$

As shown in Section 4, the parameterisation performs very well for the location of the footprint peak,  $x_{\max}$ . For the longitudinal dimension of the footprint estimate,

$x_R$ , corresponding to the ratio  $R = 90\%$ , NMSE was between 0.17 and 1.83, FB around 0.05, and CORR between 0.59 and 0.95. These values indicate a somewhat reduced performance of the parameterisation with respect to the 90% longitudinal dimension of the footprint. The cumulative footprint curves that define the stream-wise dimension are extremely flat at the 90%-level. Thus, small variations in the roll-off of the footprint function translate into relatively large deviations for this dimension. The statistics for  $R = 50\%$  are significantly better: for the simulations with a roughness length of  $z_0 = [0.01, 0.1, 0.3]$  m, NMSE for  $R = 50\%$  was reduced to values around 0.08 and CORR increased to 0.95–0.99. The according statistics for the simulations of  $z_0 = 1.0$  m improved slightly to NMSE of 1.51 and CORR of 0.65.

A tool for footprint estimation using the above parameterisation can be found at <http://footprint.Kljun.net>

## 6. Summary and Conclusions

In this study, a scaling approach for footprint functions is presented, such that, for a wide range of receptor heights and boundary-layer stabilities, and for a given roughness length, only a single non-dimensional ‘master footprint function’ results. The key variables defining this master function are the surface friction velocity, the standard deviation of the vertical velocity at the receptor, the receptor height, the height of the planetary boundary layer, the horizontal distance from the receptor location and the footprint function. Using this set, a dimensionless footprint function  $F_*$  and a dimensionless distance  $X_*$  were constructed.

The dimensionless footprint approach was tested for a large range of receptor heights, for boundary-layer stabilities ranging from strongly convective to strongly stable, and for values of the roughness length corresponding to grass surfaces up to forests. It was shown that, when plotted in this dimensionless framework and confined to certain limits ( $-200 \leq z/L \leq 1$ ,  $u_* \geq 0.2 \text{ m s}^{-1}$ , and  $z_m > 1 \text{ m}$ ), the footprint estimates for a given surface roughness collapse to an ensemble of similar curves. For footprint predictions of long-term observations within dynamically homogeneous terrain it is therefore possible to calculate the stability dependent variations in the footprint, based on only one evaluation of a suitable full footprint model that accounts for the surface characteristics and measurement height of the specific site. Applying the scaling procedure, this primary footprint estimate can be extended to any given stability condition.

To avoid the necessity for priming the scaling procedure with a full numerical footprint model (e.g., by Lagrangian stochastic diffusion or LES), the analysis was completed by proposing a parameterisation of  $F_*(X_*)$  for the ensemble of scaled footprint estimates for a broad range of receptor heights. The dependence of the scaled footprints on the roughness length was accounted for by providing suitable expressions for the dependence of the fitting parameters on the latter. The

parameterisations are easy to apply and allow ready determination of the footprint from atmospheric variables that are usually available in flux observation programs or can easily be estimated. Finally, they also allow for a quick assessment of the maximum influence location for the measurement and the streamwise dimension of the footprint.

### Acknowledgements

This research was supported by the Swiss National Science Foundation (grant 8220-067600), by the European Commission and the Swiss Ministry of Education and Science (grant 97.0136) within the TMR-project TRAPOS, and by the Swiss Commission for Technology and Innovation (KTI) in the framework of EURO-TRAC II (grants 3532.1 and 4092.1). We would like to thank Heinz Blatter, Robert Kormann, Üllar Rannik, John Wilson, and the Biomet Group (UBC) very much for their help and comments. We also thank an anonymous reviewer for drawing our attention to similarities in the approach of Hsieh et al. (2000).

### Appendix A

#### A.1. HORST AND WEIL'S MODEL

The idea of scaling the flux footprint in order to eliminate the explicit dependence on some governing parameters was already proposed by Horst and Weil (1992). They showed that

$$\Phi = \frac{z_m \overline{f^y}}{dZ/dx} = \Phi(Z/z_m), \tag{A1}$$

where  $Z(x)$  is the mean height of the plume as a function of the streamwise position.

Equation (A1) is of limited use, since  $Z(x)$  is usually not observed and must be derived using an appropriate model. However, using Van Ulden's (1978) model and assuming a vertical spread of  $\sigma_z = \sigma_w t g(t/T_L)$ ,  $T_L$  being the Lagrangian integral time scale, and Gaussian dispersion with  $g \approx 1$ , it is possible to show that

$$\frac{dZ}{dx} \approx \left(\frac{\pi}{8}\right)^{1/2} \frac{k}{[\ln(pZ/z_0) - \Psi_M(pZ/L)]} \left(\frac{\sigma_w}{u_*}\right). \tag{A2}$$

Applying our definition of  $F_*$  (Equation (6)), setting  $(1 - z_m/h)^{-1} \approx 1$  (within the surface layer), and  $\alpha_2 = 0.8 \approx 1$ , Equation (A1) can therefore be written as

$$\Phi \approx \frac{1}{k} \left(\frac{8}{\pi}\right)^{1/2} [\ln(pZ/z_0) - \Psi_M(pZ/L)] \frac{z_m \overline{f^y}}{\sigma_w/u_*}$$

$$\approx \left\{ \frac{1}{k} \left( \frac{8}{\pi} \right)^{1/2} [\ln(pZ/z_0) - \Psi_M(pZ/L)] \right\} F_*. \quad (\text{A3})$$

Similarly,  $\sigma_z \approx \sigma_w t$  and  $U(pZ) = (u_*/k) [\ln(pZ/z_0) - \Psi_M(pZ/L)]$  leads to

$$\begin{aligned} \frac{Z}{z_m} &\approx \left( \frac{2}{\pi} \right)^{1/2} \frac{k}{[\ln(pZ/z_0) - \Psi_M(pZ/L)]} \frac{\sigma_w x}{u_* z_m} \\ &\approx \left\{ \left( \frac{2}{\pi} \right)^{1/2} \frac{k}{[\ln(pZ/z_0) - \Psi_M(pZ/L)]} \right\} X_*, \end{aligned} \quad (\text{A4})$$

where the present definition of  $X_*$  (Equation (5)) was taken into account. Hence, from comparing Equations (A3) and (A4), it follows that  $\Phi = \Phi(Z/z_m)$  as given by Equation (A1) implies in our notation  $F_* = F_*(X_*)$ .

To analyse the dependence of  $F_*$  and  $X_*$  on  $z_0$ , it may be noted that in neutral conditions

$$X_{*,\max} \approx \hat{X}_{*,\max} \approx \left( \frac{Z}{z_m} \right)_{\max} \frac{1}{k} \left( \frac{\pi}{2} \right)^{1/2} [\ln(pZ) - \ln z_0], \quad (\text{A5})$$

$$F_{*,\max} \approx \hat{F}_{*,\max} \approx \Phi_{\max} k \left( \frac{\pi}{8} \right)^{1/2} \frac{1}{[\ln(pZ) - \ln z_0]}, \quad (\text{A6})$$

where  $\Phi_{\max}$  and  $(Z/z_m)_{\max}$  are the peak value and peak location of Equation (A1), with  $\Phi_{\max} \approx \text{constant} \approx 0.9$  and  $(Z/z_m)_{\max} \approx \text{constant} \approx 0.5$ . Formally, Equations (A5) and (A6) can be written as

$$\hat{X}_{*,\max} \approx A_X (B - \ln z_0), \quad (\text{A7})$$

$$\hat{F}_{*,\max} \approx \frac{A_F}{(B - \ln z_0)}. \quad (\text{A8})$$

Strictly speaking, these equations are only valid in the surface layer and for neutral conditions, but may be applied to the whole PBL and different stability conditions since  $\hat{F}_*$ ,  $\hat{X}_*$ , and the normalised footprint model of Horst and Weil (1992) are all more or less independent of  $z_m$  and  $z/L$ . Since, as opposed to LPDM-B, the dispersion is assumed Gaussian in Van Ulden (1978), the values of  $A_X$ ,  $B$ , and  $A_F$  cannot directly be inferred from Equations (A5) and (A6). However, a dependence as given by Equation (A7) must hold true for any  $\hat{X}_*$ , thus these values can be obtained by fitting Equations (A7) and (A8) to the parameterised footprint estimates of Table II.

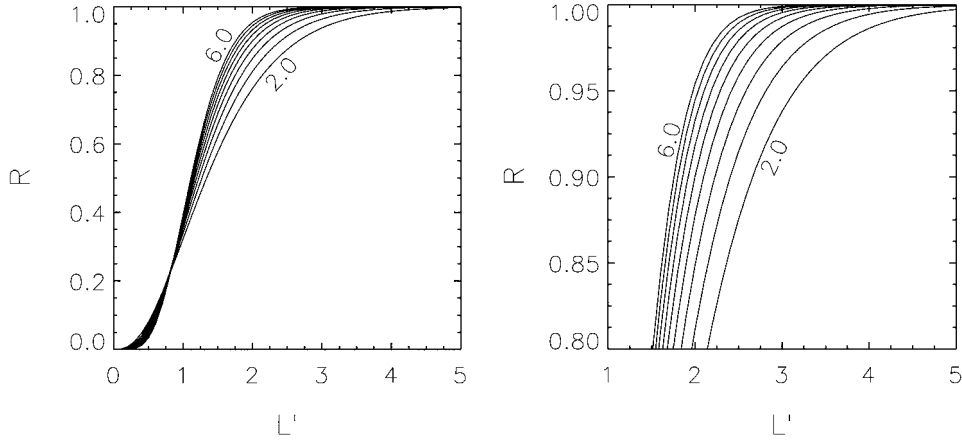


Figure A1. Ratio of the cumulative footprint as a function of a distance,  $L'$ , from the receptor for values of the footprint parameter  $b$  ranging from 2 to 6 and with a contour interval of 0.5. The right-hand panel is zoomed into the upper part of the left-hand panel.

## A.2. INTEGRATION OF FOOTPRINT PARAMETERISATION

For integration of Equation (7), the auxiliary variable,  $X' = (\hat{X}_* + d)/c$ , is introduced, with  $dX' = 1/c d\hat{X}_*$ . Thus

$$\begin{aligned} \int_{-d}^{\infty} \hat{F}_*(\hat{X}_*) d\hat{X}_* &= \int_0^{\infty} \hat{F}_*(X') dX' \\ &= \int_0^{\infty} a (X')^b \exp\{b(1 - X')\} c dX' \\ &= ac \exp(b) b^{-b} \Gamma(b), \end{aligned} \quad (\text{A9})$$

where  $\Gamma(b) \equiv \int_0^{\infty} t^{b-1} \exp(-t) dt$  is the gamma function. For the integration up to a certain distance from the receptor,  $\hat{X}_{*,R}$ , the auxiliary variable,  $L' = (\hat{X}_{*,R} + d)/c$ , is introduced. Corresponding to the above derivation

$$\begin{aligned} \int_{-d}^{\hat{X}_{*,R}} \hat{F}_*(\hat{X}_*) d\hat{X}_* &= \int_0^{L'} \hat{F}_*(X') dX' \\ &= ac \exp(b) b^{-b} \frac{1}{b} \gamma(b + 1, L'/b), \end{aligned} \quad (\text{A10})$$

where  $\gamma(b, L') \equiv \int_0^{L'} t^{b-1} \exp(-t) dt$ , i.e.,  $\gamma(b + 1, L'/b) \equiv \int_0^{L'/b} t^b \exp(-t) dt$ . Any fraction of the footprint,  $R$ , can then be determined using

$$R = \frac{\int_{-d}^{\hat{X}_{*,R}} \hat{F}_*(\hat{X}_*) d\hat{X}_*}{\int_{-d}^{\infty} \hat{F}_*(\hat{X}_*) d\hat{X}_*} = \frac{\gamma(b + 1, L'/b)}{b \Gamma(b)} = \frac{\gamma(b + 1, L'/b)}{\gamma(b + 1, \infty)}. \quad (\text{A11})$$

The ratio  $R$  reflects the percentage of the parameterised footprint included within a certain distance from the receptor. Figure A1 shows  $R$  as a function of the distance  $L'$  for different values of  $b$ .

The streamwise dimension of a footprint estimate,  $x_R$ , for a given  $z_0$ , can now be estimated by: (i) selecting a set of values for  $a$ ,  $b$ ,  $c$ , and  $d$  from Table II or using Equations (13) to (16) to compute these parameters; (ii) choosing a limit of integration, e.g.,  $R = 90\%$ ; (iii) determining the distance  $L'$  for the corresponding value of  $b$  and  $R$  from Figure A1 or by solving Equation (A11) for  $L'$  iteratively; (iv) transforming  $L'$  back to  $\hat{X}_{*,R} = L'c - d$ ; and, finally, (v) applying Equation (5) to  $\hat{X}_{*,R}$  to obtain

$$x_R \approx \hat{X}_{*,R} z_m \left( \frac{\sigma_w}{u_*} \right)^{-\alpha_1}. \quad (\text{A12})$$

## References

- de Haan, P. and Rotach, M. W.: 1998, 'A Novel Approach to Atmospheric Dispersion Modelling: The Puff-Particle Model (PPM)', *Quart. J. Roy. Meteorol. Soc.* **124**, 2771–2792.
- Hanna, S. R., Chang, J. C., and Strimaitis, D. G.: 1993, 'Hazardous Gas Model Evaluation with Field Observations', *Atmos. Environ.* **27A**, 2265–2281.
- Horst, T. W. and Weil, J. C.: 1992, 'Footprint Estimation for Scalar Flux Measurements in the Atmospheric Surface Layer', *Boundary-Layer Meteorol.* **59**, 279–296.
- Horst, T. W. and Weil, J. C.: 1994, 'How Far is Far Enough?: The Fetch Requirements for Micrometeorological Measurement of Surface Fluxes', *J. Atmos. Ocean. Tech.* **11**, 1018–1025.
- Hsieh, C. I., Katul, G., and Chi, T.: 2000, 'An Approximate Analytical Model for Footprint Estimation of Scalar Fluxes in Thermally Stratified Atmospheric Flows', *Adv. Water Resour.* **23**, 765–772.
- Kljun, N., Kormann, R., Rotach, M. W., and Meixner, F. X.: 2003, 'Comparison of the Lagrangian Footprint Model LPDM-B with an Analytical Footprint Model', *Boundary-Layer Meteorol.* **106**, 349–355.
- Kljun, N., Rotach, M. W., and Schmid, H. P.: 2002, 'A 3D Backward Lagrangian Footprint Model for a Wide Range of Boundary Layer Stratifications', *Boundary-Layer Meteorol.* **103**, 205–226.
- Kormann, R. and Meixner, F. X.: 2001, 'An Analytical Footprint Model for Non-Neutral Stratification', *Boundary-Layer Meteorol.* **99**, 207–224.
- Miyake, M.: 1965, *Transformation of the Atmospheric Boundary Layer over Inhomogeneous Surfaces*, Sci. Rep. 5R-6, University of Washington, Seattle, U.S.A.
- Raupach, M. R., Antonia, R. A., and Rajagopalan, S.: 1991, 'Rough-Wall Turbulent Boundary Layers', *Appl. Mech. Rev.* **44**, 1–25.
- Rotach, M. W.: 2001a, 'Simulation of Urban-Scale Dispersion Using a Lagrangian Stochastic Dispersion Model', *Boundary-Layer Meteorol.* **99**, 379–410.
- Rotach, M. W.: 2001b, 'Urban-Scale Dispersion Modeling Taking into Account the Turbulence and Flow Characteristics of the Roughness Sublayer', in *3rd International Symposium on Environmental Hydraulics*, Tempe, AZ.
- Rotach, M. W., Gryning, S.-E., and Tassone, C.: 1996, 'A Two-Dimensional Lagrangian Stochastic Dispersion Model for Daytime Conditions', *Quart. J. Roy. Meteorol. Soc.* **122**, 367–389.
- Schmid, H. P.: 1994, 'Source Areas for Scalars and Scalar Fluxes', *Boundary-Layer Meteorol.* **67**, 293–318.
- Schmid, H. P.: 2002, 'Footprint Modeling for Vegetation Atmosphere Exchange Studies: A Review and Perspective', *Agric. For. Meteorol.* **113**, 159–184.

- Stull, R. B.: 1988, *An Introduction to Boundary Layer Meteorology*, Kluwer Academic Publishers, Dordrecht, 666 pp.
- Van Ulden, A. P.: 1978, 'Simple Estimates for Vertical Diffusion from Sources near the Ground', *Atmos. Environ.* **12**, 2125–2129.
- Weil, J. C. and Horst, T. W.: 1992, 'Footprint Estimates for Atmospheric Flux Measurements in the Convective Boundary Layer', in S. Schartz and W. Slinn (eds.), *Precipitation Scavenging and Atmosphere – Surface Exchange*, Vol. 2, pp. 717–728.
- Wilson, J. D. and Swaters, G. E.: 1991, 'The Source Area Influencing a Measurement in the Planetary Boundary Layer: The "Footprint" and the "Distribution of Contact Distance"', *Boundary-Layer Meteorol.* **55**, 25–46.

